Toxicology and Applied Pharmacology 250 (2011) 299–311

Contents lists available at ScienceDirect

Toxicology and Applied Pharmacology

journal homepage: www.elsevier.com/locate/ytaap

The effects of deoxynivalenol on gene expression in the murine thymus

Sandra W.M. van Kol [a,c,d], Peter J.M. Hendriksen [a,d], Henk van Loveren [b,c,d], Ad Peijnenburg [a,d,*]

[a] RIKILT-Institute of Food Safety, Wageningen University and Research Centre, Wageningen, The Netherlands
[b] National Institute for Public Health and the Environment (RIVM), Bilthoven, The Netherlands
[c] Department of Health Risk Analysis and Toxicology, Maastricht University, The Netherlands
[d] Netherlands Toxicogenomics Centre, The Netherlands

ARTICLE INFO

Article history:
Received 30 June 2010
Revised 16 October 2010
Accepted 2 November 2010
Available online 11 November 2010

Keywords:
Deoxynivalenol
Lymphocyte activation
Thymus
Transcriptomics

ABSTRACT

Deoxynivalenol (DON) is a mycotoxin produced by several *Fusarium* species and is often detected in grains. Because of its high abundance, there has been a large interest in the effects of DON in animals and humans. DON is known to be immunosuppressive at high concentrations and immunostimulatory at low concentrations. The present study aimed to acquire insight into the modes of action of DON. For this, C57Bl6 mice were orally exposed to 5, 10, or 25 mg/kg bw DON for 3, 6, or 24 h and thymuses were subjected to genome-wide expression microarray analysis. Gene set enrichment analysis (GSEA) demonstrated that DON downregulated genes involved in proliferation, mitochondria, protein synthesis, and ribosomal proteins. Furthermore, GSEA showed a selective downregulation of genes highly expressed at the early precursor thymocytes stage. This indicates that early precursor thymocytes, particularly at the double-positive CD4+ CD8+ stage, are more vulnerable to DON than very early or late precursor thymocytes. There was a large overlap of genes upregulated by DON with genes previously reported to be either upregulated during T cell activation or upregulated during negative selection of thymocytes that recognize "self-antigens". This indicates that DON induces cellular events that also occur after activation of the T cell receptor, for example, release of calcium from the endoplasmatic reticulum. This T cell activation in the thymus then evokes negative selection and depletion of thymocytes, which provides a plausible explanation for the high sensitivity of the thymus for DON exposure. The expression patterns of four genes indicative for some of the processes that were affected after DON treatment were confirmed using real-time PCR. Immunocytological experiments with primary mouse thymocytes demonstrated the translocation of NFAT from the cytoplasm into the nucleus upon exposure top DON, thus providing further evidence for the involvement of T cell activation.

Introduction

Approximately 25% of the world's food crops are affected by fungal produced toxins (mycotoxins) (Rotter et al., 1996). Deoxynivalenol (DON, vomitoxin) belongs to the trichothecene mycotoxins, which are capable of generating toxic effects upon ingestion of mould-contaminated cereal grains in humans and farm animals. DON is produced by strains of *Fusarium graminearum* and *Fusarium culmorum*, which are common pathogens of cereals (Richard, 2007). Although DON is not as toxic as other trichothecenes such as T-2 toxin, it is considered as one of the most common toxic contaminants of wheat, corn, and barley. DON remains stable during storage and processing and does not degrade at high temperature (Rotter et al., 1996). Orally dosed mice show a peak uptake of DON within 30 min along with distribution in plasma and many tissues. In mice orally exposed to 25 mg/kg bw DON, the toxin was detected after 30 min in several organs including spleen and thymus with a rapid decrease to concentrations close to control levels occurring over 24 h (Azconaolivera et al., 1995; Pestka et al., 2008). DON undergoes de-epoxidation by gut-microflora and is conjugated to glucuronides in the liver. Resultant metabolites are excreted from the body via urine and feces (Pestka, 2007; Amuzie et al., 2008).

DON has a major effect on actively dividing cells including bone marrow, spleen, and thymus cells, and, as a consequence, it has a large effect on the immune system (Pestka et al., 2004). DON induces thymus atrophy at concentrations above 10 mg/kg fed to BALB/c mice daily for a week. Spleen weight was decreased, but less then thymus weight (Robbana-Barnat et al., 1988). This finding was one of the first indications that the immune system is a primary target of DON. The effects of exposure to DON can be either immunosuppressive or immunostimulatory, depending on the length of exposure and dosage concentration. Low doses of DON promote the expression of various cytokines and chemokines *in vitro* and *in vivo*, which involves transcriptional or post-transcriptional mechanisms (Zhou et al., 1997; Kinser et al., 2004; Pestka et al., 2004). Relevant immunostimulatory effects include an increase in

* Corresponding author. Ad Peijnenburg RIKILT-Institute of Food Safety, Wageningen UR, PO Box 230, 6700 AE Wageningen, The Netherlands. Fax: +31 317 417717.
E-mail address: Ad.Peijnenburg@wur.nl (A. Peijnenburg).

0041-008X © 2010 Elsevier Inc. Open access under the Elsevier OA license.
doi:10.1016/j.taap.2010.11.001

levels of serum IgA and IgE, which are mediated by cytokines excreted by macrophages and T cells. High doses of DON cause rapid apoptosis of leukocytes that manifests itself as immunosuppression. Extremely high doses can cause a shock-like death in mice. When administered intraperitoneally, the LD50 value for mice ranges from 49 to 70 mg/kg bw, and when administered orally, from 46 to 78 mg/kg bw (Forsell et al., 1987; Pestka, 2007).

Kinser et al. (2004) performed a gene expression study on spleens of mice orally exposed to 25 mg/kg DON for 2 h. They found many genes altered by acute DON exposure. Most of the upregulated genes were immediate early genes involved in immunity and inflammation. A drawback of this study was the low number of genes on the microarrays. So far, little data are available on the effect of DON on gene expression in the thymus. The thymus is an important organ where T cell differentiation, selection, and maturation occur. During T cell selection, lymphocytes expressing receptors that recognize foreign proteins are positively selected and lymphocytes that react to self-antigens are negatively selected and go into apoptosis (Starr et al., 2003). Disturbance of the development of thymocytes has a major effect on the defence system.

The aim of the present study was to obtain a better insight in the mechanism of action of DON in the mouse thymus using whole genome microarrays. Male C57Bl6 mice were gavaged with different doses of DON and were sacrificed after 3, 6, and 24 h. DON treatment caused a rapid induction of gene expression. The effect of DON on the number of affected genes ($\geq 1.5\times$ up- or downregulated, p value <0.01) was highest after 3 h for the lowest and middle dose and much lower after 24 h, indicating a reversible effect. In contrast, the highest concentration of 25 mg/kg DON had an irreversible effect on the number of genes affected. The biological interpretation of the microarray data led to the hypothesis that DON induces thymocyte depletion via induction of the T cell activation response that is quickly followed by negative selection of thymocytes.

Materials and methods

Animals. The DON *in vivo* study was performed with 7-week-old male C57BL/6 mice that were obtained from Harlan (Horst, The Netherlands). Animals were kept at a housing temperature of 22 °C and at a relative humidity of 30–70%. Lighting cycle was 12-h light and 12-h dark. The treatment protocol was approved by the ethical committee for animal experiments at Wageningen University, Wageningen, The Netherlands.

Treatment. The experiment included 60 mice, which were randomly divided into 12 different groups. DON was dissolved in ethanol and then diluted with endotoxin-free water. The amount of ethanol was kept the same for all mice (2.5 μl/g bw). The mice obtained one dose of DON by oral gavage (5, 10, or 25 mg/kg bw). The control groups per time point received only the vehicle ethanol. DON or vehicle was administered to one mouse each every 10 min to keep the treatment times constant. After 3, 6, or 24 h, the mice were sacrificed by cervical dislocation under isoflurane anesthesia. The thymus was isolated, immediately frozen in liquid nitrogen, and kept frozen until further gene expression analysis. The doses used in this study were chosen based on literature. The lowest dose used (5 mg/kg DON) was chosen, because it resembles the total daily consumption of DON in mice digesting a diet of 25 ppm DON. This level has been shown to result in an increase of circulating IgA and changes in the expression levels of different genes encoding cytokines, such as Il6 and TNFα, in the spleen (Azconaolivera et al., 1995; Amuzie et al., 2008). The highest dose of 25 mg/kg DON is one-third of the LD50 of DON in mice (Azconaolivera et al., 1995).

RNA isolation. Thymuses were homogenized in 1 ml of TRIzol reagent (Invitrogen, Breda, The Netherlands) per 50–100 mg tissue, using a homogenizer (Pro Multi-Gen 7, PRO Scientific, Oxford, CT). Subsequently, RNA was isolated following supplier's instructions. After purification using the RNeasy Mini Kit (Qiagen, Venlo, The Netherlands), integrity, purity, and concentration were assessed by automated gel electrophoresis (Experion, Biorad, Veenendaal, The Netherlands) and spectrophotometrically at wavelengths of 230, 260, and 280 nm.

Preparation of labeled cRNA and microarray hybridization. One microgram of each individual RNA sample was amplified using a low RNA Input Fluorescent Linear Amplification Kit (Agilent Technologies, Amstelveen, The Netherlands). Subsequently, the common reference sample, Universal Mouse Reference RNA (Stratagene, Amsterdam, The Netherlands), was labeled with Cy3 and the thymus RNAs were labeled with Cy5. The labeled cRNAs were purified (QIAquick spin columns, QIAGEN, Venlo, The Netherlands) and 1 μg of each sample was hybridized to 4×44 K whole genome mouse oligo microarrays (G4122F, Agilent) according to manufacturer's instructions (two-color microarray-based gene expression analysis, Agilent). After a 17-h incubation period, slides were washed using various dilutions of SSPE (sodium chloride, sodium phosphate, EDTA) buffer according to the protocol provided by Agilent. Arrays were scanned using an Agilent microarray scanner (G2565B). The fluorescent readings from the scanner were converted to quantitative files using Feature Extraction 9.1 software (Agilent Technologies). Quality check of the arrays was done using software package LimmaGUI in R version 2.3.1. Four samples were removed from the analysis due to technical failure. Data were imported in GeneMaths XT 1.5 (Applied Maths, St. MartensLatem, Belgium), and spots with signal intensities below two times background were excluded from subsequent analysis. Corrected data were normalized and adjusted for random and systematic error (Pellis et al., 2003).

Overview of significantly up- and downregulated genes. Significance analysis of microarrays (SAM) analysis was applied to detect significantly affected genes for each treatment using the two-class unpaired comparison (Tusher et al., 2001). The False Discovery Rate was set to <0.5%. No additional filtering on a threshold for up- or downregulation was applied. Evaluation of the outcome of the SAM results showed that the minimal ratio for up- or downregulation was 1.5.

Hierarchical clustering. Hierarchical clustering was done with the programs Cluster (uncentered correlation; average linkage clustering) and Treeview (Eisen et al., 1998).

Metacore. Metacore (GeneGo, St. Joseph, MI) is an online software program that provides, among other options, pathway analysis of microarray data. Groups of co-clustering genes were analyzed for overrepresentation of genes from signaling and metabolic pathways based on hypergeometric distribution (Ekins et al., 2006). Pathways with a p value$<10^{-5}$ were considered significant.

GSEA. Gene set enrichment analysis (GSEA) was performed to discover the differential expression of biologically relevant sets of genes that share common biological function or regulation (Subramanian et al., 2005). GSEA has the advantage that no initial filtering is applied to the data set to select for significantly differentially expressed genes. GSEA first ranks all probe sets based on fold changes (algorithm signal to noise) in expression between a treatment and the control. Subsequently, by using pre-defined sets of associated genes based on prior biological knowledge, GSEA calculates whether sets as a whole are enriched at the top or bottom of the fold change-based ranking list, or randomly distributed (Subramanian et al., 2005). This enables detection of significantly affected gene sets, while the fold change of expression of the individual genes can be relatively modest. GSEA was performed for all treatment groups vs. controls at same time point. Gene sets with a p

value < 0.05 and an FDR value < 0.25 were considered being significantly regulated. Up- and downregulation of significant gene sets were visualized with heap maps. The *p* values were converted into *Z* values to enable clustering. Gene sets obtained positive or negative *Z* values when up- or downregulated, respectively. Hierarchical clustering was done as described above.

For GSEA, five collections of gene sets were used:

1. Cell cycle: data taken from supplemental data of Whitfield et al. (2002) and Bar-Joseph et al. (2008). In these studies, cells were first synchronized at the G0 cell stage and then stimulated to retain the cell cycle. Microarray analysis was performed to detect genes upregulated during certain cell cycle stages. Up- or downregulation of these gene sets is indicative for a higher or lower proliferation rate.
2. Gene ontology: gene sets (mouse gene symbols) were downloaded from the Gene Ontology Consortium (http://www.geneontology.org/). This collection contains gene sets related to general cellular processes.
3. Lymphocyte signature database: gene sets were taken over from Shaffer et al. (2001). A proportion of these gene sets are based on results from expression profiling studies on lymphocytes.
4. Tissue-specific blood cell types: data taken from Su et al. (2004), Lyons et al. (2007), Du et al. (2006), and Hoffmann et al. (2003). This collection contains gene sets that are specifically highly expressed in certain blood cell types.
5. TOX TFS target genes: contains gene sets related to (1) toxic action of compounds or (2) target genes of toxicity-related transcription factors. These gene sets were deduced from microarray data.

Molecular concepts analysis. Molecular concepts analysis enables to visualize networks in which the overlap between gene sets based on co-occurrence of genes are shown (Rhodes et al., 2007). This overlap was calculated based on the genes that were responsible for a gene set to be significantly affected. For this, either the top 20% of the genes being upregulated or the top 20% of the genes being downregulated was used. Gene set selection for molecular concepts mapping was more stringent than used for making heat maps. Gene sets were selected on a *p* value <0.01 in combination with an FDR value <0.25 according to GSEA statistics. In addition, gene sets containing ≤ 8 genes were excluded from the analysis. After applying these criteria, 74 upregulated and 80 downregulated gene sets remained. The significance of overlap between the gene sets was calculated based on the binomial distribution using Venn-Mapper (Smid et al., 2003). Gene sets showing significant overlap (*Z* value >2.72 that is equal to $p<0.0001$) were connected in a network that was visualized using Cytoscape (Shannon et al., 2003).

Genes from the gene sets with high overlap (high *Z* values) were clustered close to each other. Gene sets within a same cluster are expected to have a similarity in biological effects. These gene sets were merged, and heat maps showing the effects of all treatments on the genes of those merged gene sets were generated using GSEA.

Isolation of primary thymocytes. Seven-week-old male C57BL/6 mice were obtained from the breeding colony of Wageningen University and sacrificed by CO_2 without any preceding treatment. The protocol was approved by the ethical committee for animal experiments at Wageningen University. The thymus was excised aseptically and collected in 3 ml RPMI 1640 medium, containing HEPES (Invitrogen Life Science, Breda, The Netherlands) with 10% heat-inactivated Fetal Bovine Serum (FBS) (Invitrogen Life Science), 100 U/ml Penicillin, and 100 μg/ml streptomycin (Invitrogen Life Science) (standard medium). The thymus was gently pressed through a 70-μm nylon cell strainer (Falcon, Franklin Lakes, NJ) to prepare a single-cell suspension. After centrifuging (10 min, 1200 rpm, 4 °C), the cell suspension was resuspended in 5 ml of red blood cell lysis buffer (NH_4Cl 155 mM, $KHCO_3$ 10 mM, EDTA 1 mM; pH 7.4) and incubated for 5 min on ice. Cells were washed with standard medium (10 min, 1200 rpm, 4 °C) and counted with a Coulter Counter (Beckman Coulter, Woerden, The Netherlands). The concentration of the cell suspensions was adjusted to 0.25×10^6 cells/ml using standard medium.

Immunocytology. Freshly prepared DON solutions in absolute ethanol were diluted in standard medium and added to the primary thymocyte cultures (in 6-well plates) to a final concentration of 0.5 μM DON. The final ethanol concentration was. Upon exposure for 1 h at 37 °C, primary thymocytes were immobilized on poly-L-lysine-coated slides (Menzel-Glaser, Braunschweig, Germany) using mild cytospin centrifugation (6 min at 600×*g*) followed by incubation in 4% paraformaldehyde with 0.025% glutaraldehyde in PBS for 30 min. After blocking cells with 1% BSA and 0.01% Triton-X 100 in PBS for 45 min, they were washed in 0.1% acetylated BSA (AUrion, Wageningen,NL) in PBS and incubated overnight at 4 °C with 1/100 dilution of a primary antibody directed against NFATC1 (Santa Cruz Biotechnology) in 0.1% acetylated BSA in PBS. After extensive washing in 0.1% acetylated BSA in PBS, the cells were incubated with 1/300 goat anti-mouse–IgG1–FITC secondary antibody for 120 min at 37 °C. Slides were washed in PBS, mounted in Vectashield containing DAPI (Vectashield, Amsterdam, The Netherlands), and imaged with an LSM510 (Carl Zeiss, Jena, Germany) confocal microscope.

Images of DAPI and FITC were acquired with 405- and 488-nm excitation in multitrackmode to prevent cross-signals. Images were obtained with 420- to 480-nm BP filter for DAPI and 505- to 530-nm BP filter for FITC with a 63× Plan Apochromat objective NA1.4 to obtain high *z*-resolution (<1.0 μm optical slice).

Real time RT-PCR. Expression levels of 4 genes in all samples used for microarray analysis were measured by means of real time RT-PCR. These genes were selected on the basis of the outcome of the microarray data analysis. PCR primers were designed using Beacon designer 7.00 (Premier Biosoft International, Palo Alto, CA). Primers for CD80 were sense 5′-CGACTCGCAACCACACCATTAAG-3′ and antisense 5′-CCCGAAGGTAAGGCTGTTGTTTG-3′, for CD86 sense 5′-TCACAAGAAGCCGAATCAGCCTAG-3′, and antisense 5′-GCTCTCACTGCCTTCACTCTGC-3′ for ATF3 sense 5′-ATAGAAGAGGTCCGTAAGGCAAGG-3′ and antisense 5′-TTATTACAGCAAACACAGCAACACAAG-3′ and for Ccl4 sense 5′-CCCACTTCCTGCTGTTTCTCTTAC-3′ and antisense 5′-GCTCAGTTCAACTCCAAGTCACTC-3′. One microgram RNA was converted into cDNA using the iScript cDNA Synthesis Kit (bio-Rad). One sample was taken along without reverse transcriptase to examine the presence of DNA (-RT reaction). RT-PCR reactions were performed in triplicate, using the Bio-Rad MyiQ Single-Color Real-Time PCR Detection System (Veenendaal, The Netherlands). The reaction mixture contained 2 μl of cDNA and 23 μl of iQ SYBR green super mix consisting of reaction buffer with dNTPs, iTaq DNA polymerase, SYBER green I and fluorescein (Bio-Rad-170-8882). The reaction mixtures were incubated for 3 min at 95 °C, followed by 40 cycles of amplification. The PCR settings were as follows: denaturation 15 s at 95 °C, annealing 45 s at 60 °C, and extension 1 min at 65 °C, with single fluorescence acquisition at 65 °C after each cycle. *Hprt1* (sense 5′- TGGGCTTACCTCACTGCTTTCC-3′ and antisense 5′- CCTGGTTCATCATCGCTAATCACG-3′) and *Actb* (sense 5′- AGC CAT GTA CGT AGC CAT CCA-3′ and antisense 5′- TCT CCG GAG TCC ATC ACA ATG-3′) were selected as reference genes since these were not differentially regulated by DON as judged from the microarray results. Normalization was performed using the reference gene, and the relative expression of the target genes was calculated. Data were analyzed by MyQ5 software (Bio-Rad).

Results

Mice were gavaged with three different doses (5, 10, or 25 mg/kg bw) of DON for three time periods (3, 6, and 24 h) and the thymus was

Table 1
Relative thymus weight (mg/g bw) of mice treated with DON. Mice were treated with 0, 5, 10 and 25 mg/kg DON for 3, 6 and 24 hours.

Time	DON (mg/kg bw)	Mouse weight (g)	SD	Absolute thymus weight (mg)[a]		Relative thymus weight (mg/g BW)[a]	
3 h	0	23,7	2.4	74,4	8.6	3,14	0.16
	5	22,8	1.1	74,2	15.1	3,25	0.73
	10	23,84	1.8	74,6	11.8	3,13	0.55
	25	23,18	0.7	73,5	16.7	3,17	0.66
6 h	0	23,16	1.3	76,4	8.7	3,3	0.21
	5	22,94	1.9	78,6	30.0	3,43	1.10
	10	21,46	3.0	78,4	20.4	3,66	0.78
	25	24,68	2.7	79,8	18.6	3,24	0.42
24 h	0	23,74	2.6	83,0	10.7	3,5	0.46
	5	22,72	0.8	71,6	16.2	3,15	0.77
	10	22,68	1.3	76,1	21.4	3,36	0.82
	25	20,78	1.5	48,8**	10.3	2,35*	0.46

[a]: *: P<0.01; **: P<0.001 (Student's T test).

isolated and subjected to microarray analysis. Treatment with 25 mg/kg bw DON for 24 h resulted in a decrease of the ratio between thymus weight and body weight (Table 1). As determined by SAM, treatment with 5 mg/kg DON resulted in 634 genes to be significantly affected within 3 h already. At this dose, the number of affected genes decreased to 65 after 6 h and to 0 genes after 24 h. This decrease of number of affected genes was also observed for the treatment with 10 mg/kg bw DON, i.e., 713, 117, and 23 genes affected after 3, 6 and 24 h, respectively. This indicates that after exposure to 5 and 10 mg/kg DON, the mice recovered over time. This pattern was not observed for the highest dose of 25 mg/kg, which is one-third of the LD50. This resulted in a constant number of affected genes, i.e., 924, 1124, and 1707 after treatment for 3, 6, or 24 h, respectively.

Hierarchical clustering and pathway analysis

Fig. 1 shows a hierarchical clustering for genes that were at least 2.6-fold up- or downregulated (2log ratio of>|1.4|) vs. the average of the controls in≥3 of the 32 arrays (selection of 2026 spots representing 1555 genes). Six clusters can be distinguished. Cluster 1 contains genes that were mainly upregulated by 10 and 25 mg/kg DON after 24 h. A large group of genes (cluster 2) were highly upregulated by each of the DON doses within 3 h already. These genes were also upregulated after 6 and 24 h by the highest DON dose but were much less or not upregulated anymore by the lower doses at these time points. The genes within cluster 3 were upregulated after 24 h and variably expressed in the 3- and 6-h control samples. Cluster

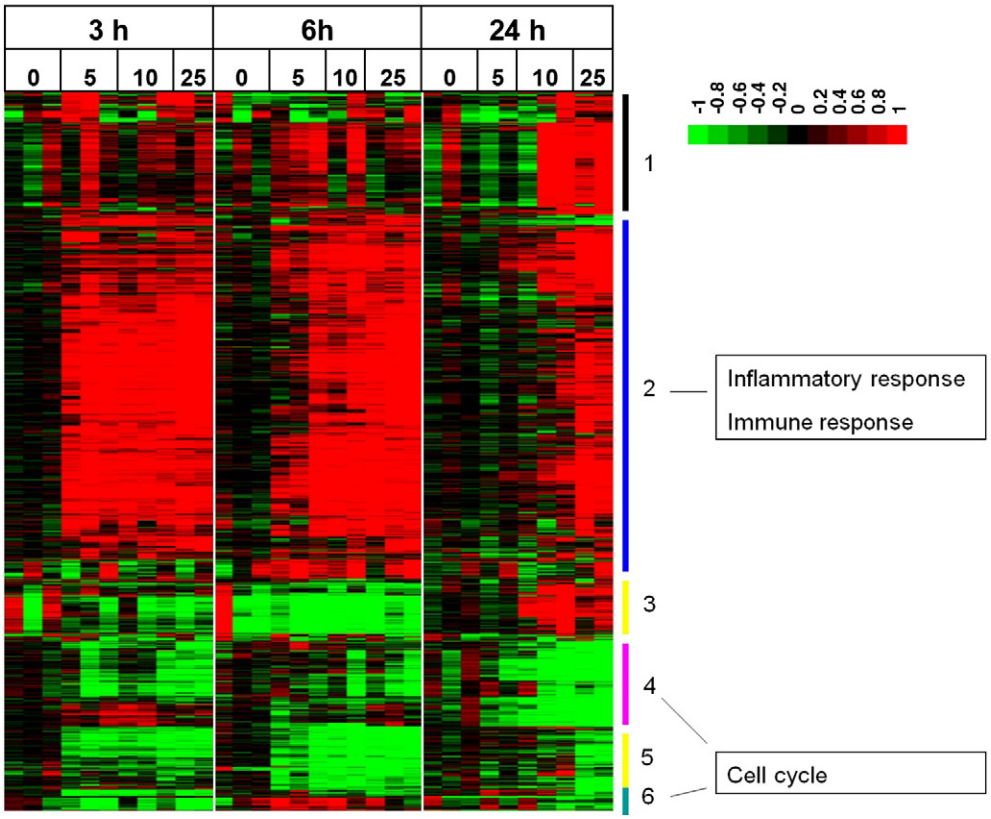

Fig. 1. Hierarchical clustering of DON-affected genes. The heat map shows 2026 spots representing 1555 genes that were ≥2.6 times up- or downregulated vs. the average of the control in at least 3 out of 32 arrays. Gene expression levels are indicated by colors, red: upregulation, black: no regulation, and green: downregulation compared to the average of the control. Basically, six clusters of genes can be distinguished based on gene expression levels. The affected biological processes are indicated to the right of the corresponding clusters.

4 contains genes highly downregulated after exposure for 24 h. A proportion of these genes were downregulated at 3 and 6 h, whereas other genes of this cluster were upregulated at 3 h. Cluster 5 contains genes downregulated after 3 and 6 h of treatment but less downregulated after 24 h. The genes of cluster 6 were first downregulated after 3 h and upregulated after 6 h.

Metacore analysis of the genes from the individual clusters revealed a clear difference in functionality between the genes of cluster 2, 4, and 6. Genes from cluster 2 were involved in immune pathways, including the IL-17 and IL-1 signalling pathway (p value: 10^{-13} and 10^{-12}, respectively) and the Toll-like receptor pathway (p value: 10^{-9}). The genes that were downregulated at the latest time point (cluster 4) were part of several cell cycle pathways, such as those involved in metaphase checkpoint control and APC-mediated cell cycle regulation (p value: 10^{-25} and 10^{-20}, respectively). Genes from cluster 6 were involved in the cell cycle as well. The two most significant pathways were "start of DNA replication in early

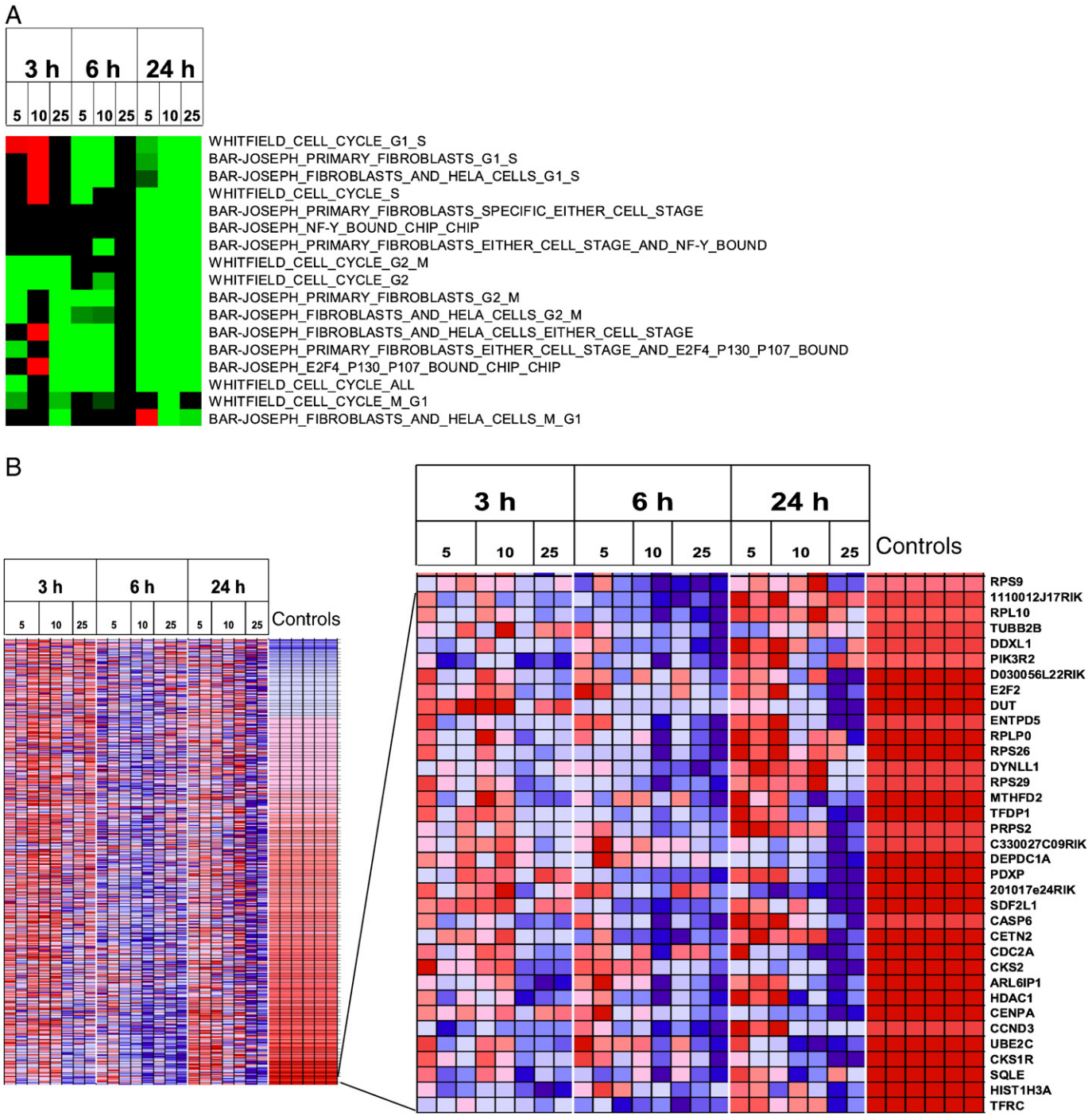

Fig. 2. DON treatment affects gene sets indicative for proliferation. (A) Overview of the effect of DON on gene sets specifically upregulated during a cell cycle stage. Green indicates downregulation and red upregulation compared to controls. Black indicates no effect. Genes highly expressed during the G1–S phase of the cell cycle were upregulated after 3 h and downregulated after 6- and 24-h exposure to DON. (B) Heat map of the genes from the merged proliferation related gene sets of Supplementary Fig. 2. The heat map contains 2log ratios of treatment vs. the average of the control at the same time point. For visualization, six columns containing zeros were added, representing the relative expression of the control samples. Colors represent relative gene expression levels, blue indicates low expression, red indicates high expression.

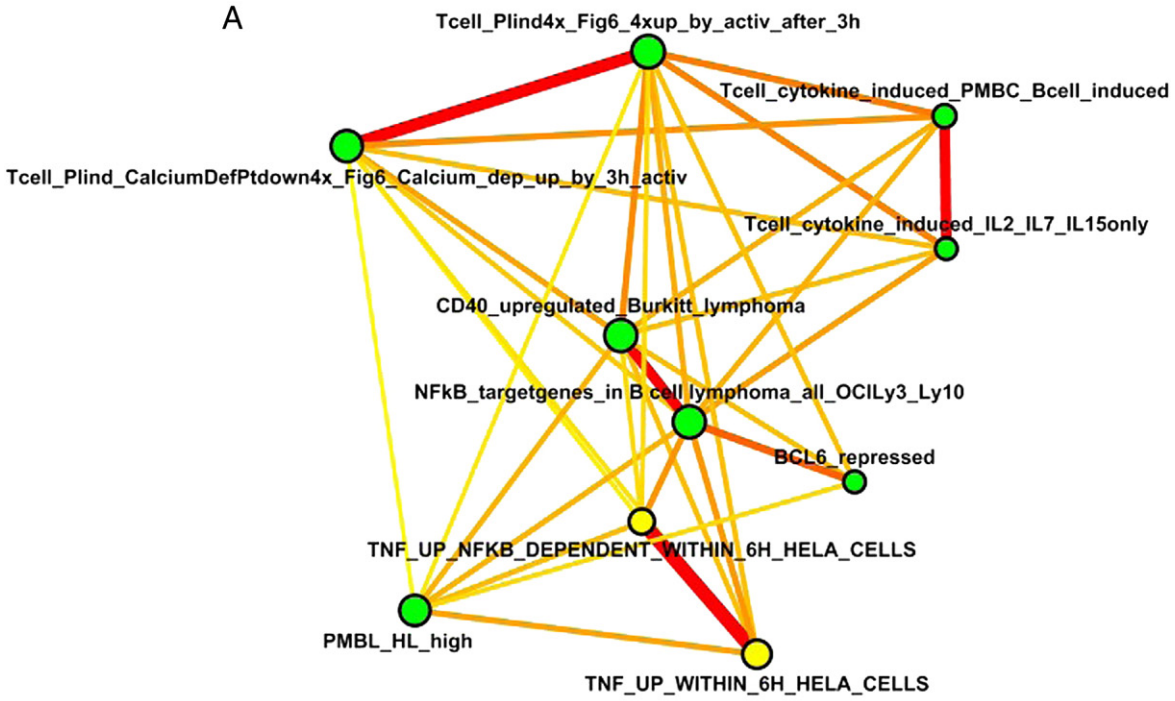
A
Tcell_Plind4x_Fig6_4xup_by_activ_after_3h
Tcell_cytokine_induced_PMBC_Bcell_induced
Tcell_Plind_CalciumDefPtdown4x_Fig6_Calcium_dep_up_by_3h_activ
Tcell_cytokine_induced_IL2_IL7_IL15only
CD40_upregulated_Burkitt_lymphoma
NFkB_targetgenes_in B cell lymphoma_all_OCILy3_Ly10
BCL6_repressed
TNF_UP_NFKB_DEPENDENT_WITHIN_6H_HELA_CELLS
PMBL_HL_high
TNF_UP_WITHIN_6H_HELA_CELLS

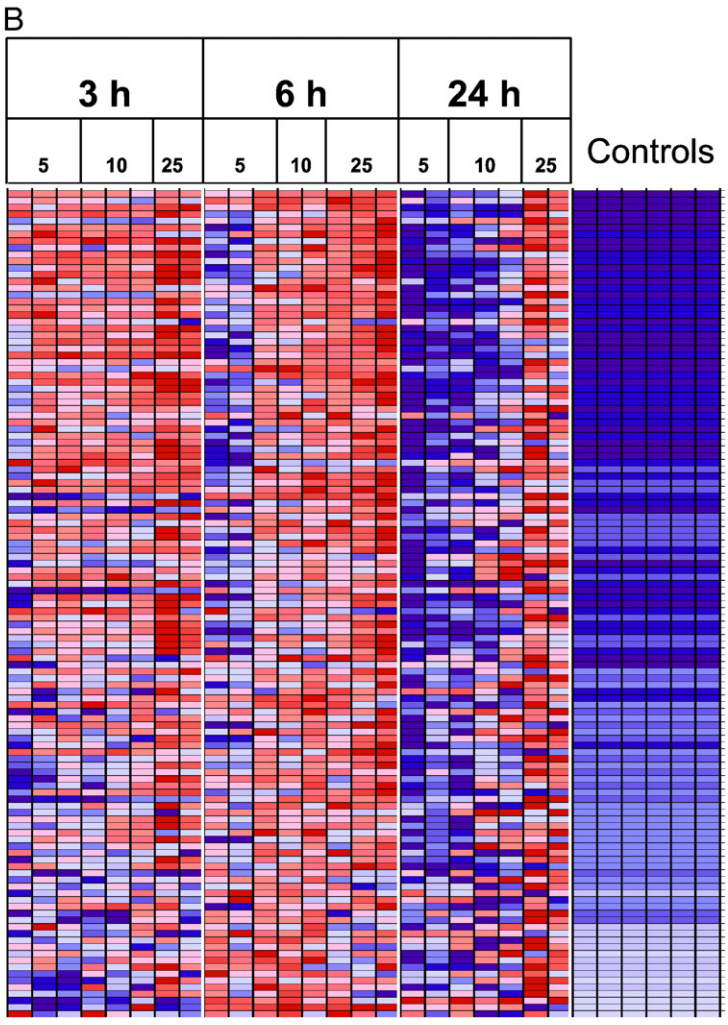
B
3 h
6 h
24 h
5
10
25
5
10
25
5
10
25
Controls

S phase" (p value: 10^{-6}) and "the metaphase checkpoint" (p value: 10^{-6}). Metacore analysis of genes from clusters 1, 3, and 5 did not result in significantly regulated pathways.

Gene set enrichment analysis (GSEA) and molecular concepts mapping

Gene set enrichment analysis was used for the identification of gene sets affected by DON in order to unravel mechanisms of DON toxicity. This enables the comparison of our results with results already published in literature or derived from microarray studies.

A three-step approach was followed. Firstly, GSEA was performed on each of the nine treatment groups in relation to the control samples at the same time point. Up- and downregulation of significant gene sets were visualized in heat maps enabling comparison between the treatment groups. This resulted in 264 gene sets, obtained from five gene set collections, that were significantly affected by at least one treatment. Secondly, molecular concepts mapping was performed to further facilitate the biological interpretation. This provided a visualization of the overlap in genes among the significant gene sets from the combined gene set collections. Based on clusters of highly similar gene sets, the main biological events were elucidated. Molecular concepts mapping was performed for one treatment: 6-h exposure to 10 mg/kg. This treatment was selected since nearly all gene sets affected by any treatment were also affected by this dose at this time point. Thirdly, gene sets showing high overlap according to molecular concepts mapping were merged. The rationale for this step was that a high overlap is indicative for comparable biological effects. Heat maps were made to investigate the expression of the individual genes of merged gene sets for all treatment groups.

The results of the molecular concepts mapping for all gene sets are shown in Supplementary Fig. 1. The gene sets upregulated by 6-h exposure to 10 mg/kg DON clustered into five themes: lymphocyte activation, inflammatory response, blood cell infiltration, late precursor T cells, and a combination of cell adhesion and cytoskeleton (Supplementary Fig. 1A). The gene sets downregulated by the same treatment yielded five clusters as well: mitochondrion, ribosome, cytoplasm/nucleus, early-precursor T cells, and proliferation (Supplementary Fig. 1B).

Proliferation

A molecular concepts visualization of the gene sets that are indicative for the proliferation rate is shown in Supplementary Fig. 2. The downregulation of the cell cycle related gene sets indicates a major inhibiting effect of DON on the proliferation. These gene sets include genes that are specifically upregulated during a particular cell cycle phase (Whitfield et al., 2002; Bar-Joseph et al., 2008). Interestingly, genes upregulated during the G1–S phase of the cell cycle were upregulated after 3-h treatment with 5 μg/kg and particularly 10 μg/kg DON (Fig. 2A). This indicates that 10 mg/kg DON rapidly stimulates entry of cells into the G1–S phase of the cell cycle but inhibits cell division shortly thereafter. A heat map of the expression of the genes of the merged proliferation-related gene sets is given in Fig. 2B. This figure (upper part of heat map at the left) shows that many of the cell cycle genes were temporarily upregulated during the first 3 h.

T cell activation

As shown in Fig. 3A, genes that are upregulated in T lymphocytes during the T cell activation response are also upregulated by DON. These gene sets include NFkB, CD40, Fos, and Jun (Supplementary Fig. 3), which are well-known for being induced by T cell activation (Gwack et al., 2007). In agreement with this, NFkB target genes and CD40 upregulated genes are also induced by DON (Fig. 3A). These T cell activation-related genes were upregulated within 3 h. These genes remain highly upregulated after 24 h for the highest dose of DON but return within 24 h close to control levels for the lowest and middle dose of DON (Fig. 3B).

Inflammatory response, blood cell infiltration, cell adhesion–cytoskeleton

DON upregulated of many inflammatory response-related gene sets including chemokine activity, chemotaxis, inflammatory response, and acute phase response (Supplementary Fig. 4A). These gene sets contained many cytokine-related genes (Supplementary Fig. 4B). The upregulation of gene sets such as dendritic cells, monocytes, and polymorphonuclear leucocytes (Supplementary Fig. 5A and C) indicates an infiltration of blood cells with phagocytotic ability. One other cluster of gene sets upregulated by DON was related to cell adhesion and cytoskeleton (Supplementary Fig. 6A). The expression pattern over time of inflammatory response, blood cell infiltration, and cell adhesion–cytoskeleton genes was remarkable similar to that of the T cell activation-induced genes (Supplementary Figs. 4B, 5B, D and 6B).

Precursor T lymphocytes

Genes highly expressed in either the very earliest precursor T lymphocytes stage (DN2) or the late precursor stages ($CD4^+$ or $CD8^+$) were upregulated by DON treatment, while genes highly expressed in early precursor cells of the double-positive stage ($CD4^+$ and $CD8^+$) were downregulated by DON (Supplementary Fig. 7A, B, and D). Genes highly expressed in early precursor stages DN3 and DN4 are upregulated at 3 h and downregulated at 6 and 24 h (Supplementary Fig. 7A and B). The downregulation of the early precursor marker genes and the upregulation of the late precursor marker genes were most apparent at 6 h for all doses and at 24 h for the highest dose of DON (Fig. 4A and B, Supplementary Fig. 7C and E). After 24 h, gene expression in thymuses of mice exposed to 5 and 10 mg/kg DON was for the most part recovered. In marked contrast, the effects of 24-h exposure to 25 mg/kg DON were more severe than those after 3 and 6 h (Fig. 4, Supplementary Fig. 7C and E). These findings indicate that the early precursor T lymphocytes that are at or close to the double-positive stage are most sensitive for DON treatment.

Mitochondrion, ribosome, cytoplasm/nucleus

Genes encoding proteins for cellular components as mitochondria, ribosomes, and cytoplasm/nuclei were downregulated by DON. The molecular concepts picture for ribosomes also contains gene sets related to mRNA splicing, nucleosome, protein synthesis, and ribosomal RNA binding, indicating that genes involved in the entire route for mRNA modification to protein translation were downregulated (Fig. 5A). As shown in the heat map of Fig. 5B, this

Fig. 3. DON upregulates gene sets related to lymphocyte activation. (A) Molecular concepts visualization of gene sets containing genes upregulated during T cell activation. These gene sets were upregulated after 6-h exposure to 10 mg/kg DON. The size of the nodes corresponds to the number of genes of the gene set, and the width and boldness of the connecting lines indicate the degree of overlap between the gene sets. The color of the nodes corresponds to the gene set collection from which the gene sets were taken. Green: lymphocyte signature database; yellow: TOX TFS target genes. (B) Heat map of genes involved in T lymphocyte activation. The heat map contains 2log ratios of treatment vs. the average of the control at the same time point. For visualization, six columns containing zeros were added, representing the relative expression of the control samples. Colors represent relative gene expression levels, blue indicates low expression, red indicates high expression. The picture for all genes including gene symbols is provided in Supplementary Fig. 3. T cell activation genes were upregulated within 3 h and remained upregulated after 24-h treatment with 25 mg/kg bw DON. Most T cell activation-related genes were not upregulated anymore after 24-h treatment with 5 and 10 mg/kg bw DON.

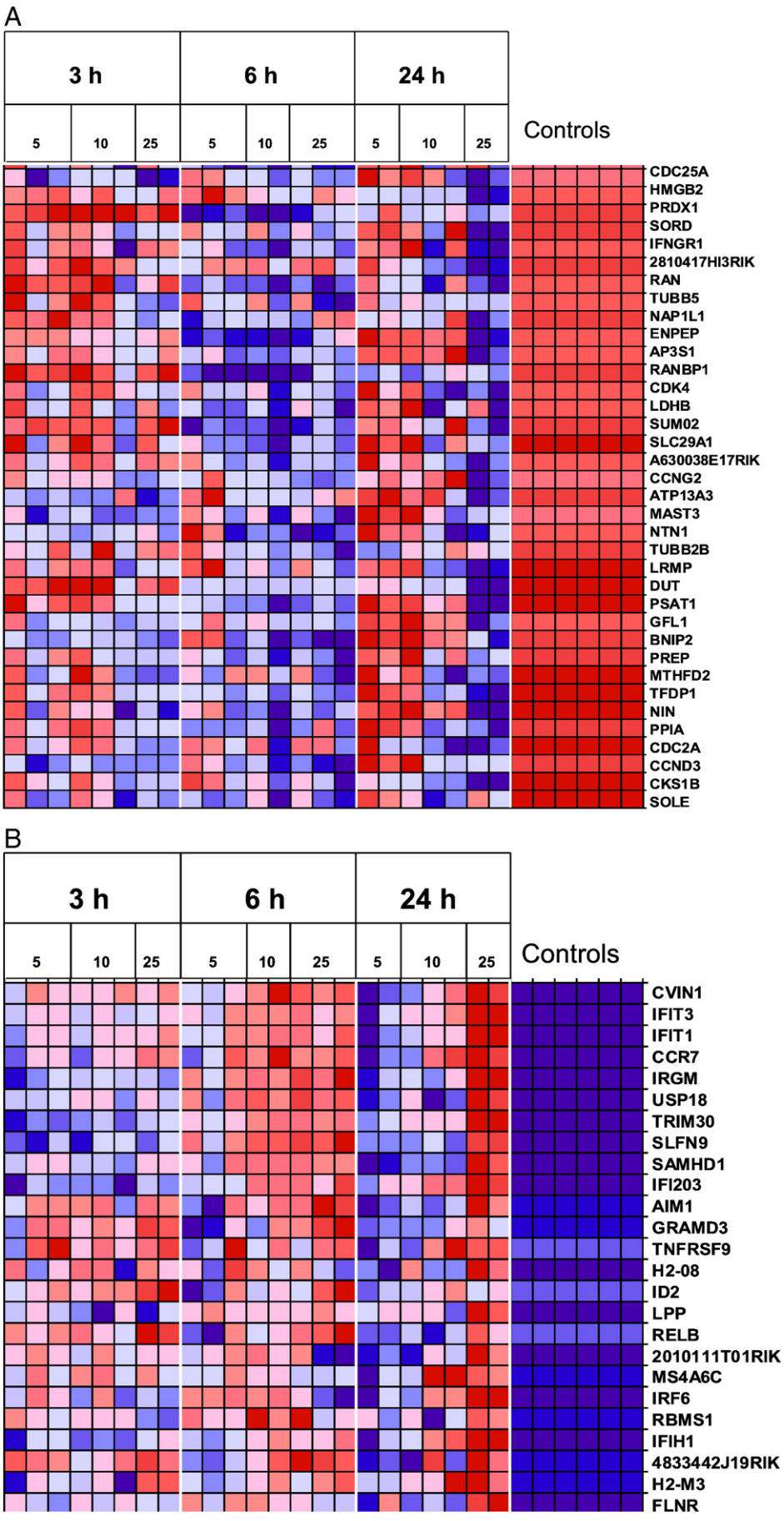
A
3 h
6 h
24 h
5
10
25
5
10
25
5
10
25
Controls
CDC25A
HMGB2
PRDX1
SORD
IFNGR1
2810417HI3RIK
RAN
TUBB5
NAP1L1
ENPEP
AP3S1
RANBP1
CDK4
LDHB
SUM02
SLC29A1
A630038E17RIK
CCNG2
ATP13A3
MAST3
NTN1
TUBB2B
LRMP
DUT
PSAT1
GFL1
BNIP2
PREP
MTHFD2
TFDP1
NIN
PPIA
CDC2A
CCND3
CKS1B
SOLE
B
3 h
6 h
24 h
5
10
25
5
10
25
5
10
25
Controls
CVIN1
IFIT3
IFIT1
CCR7
IRGM
USP18
TRIM30
SLFN9
SAMHD1
IFI203
AIM1
GRAMD3
TNFRSF9
H2-08
ID2
LPP
RELB
2010111T01RIK
MS4A6C
IRF6
RBMS1
IFIH1
4833442J19RIK
H2-M3
FLNR

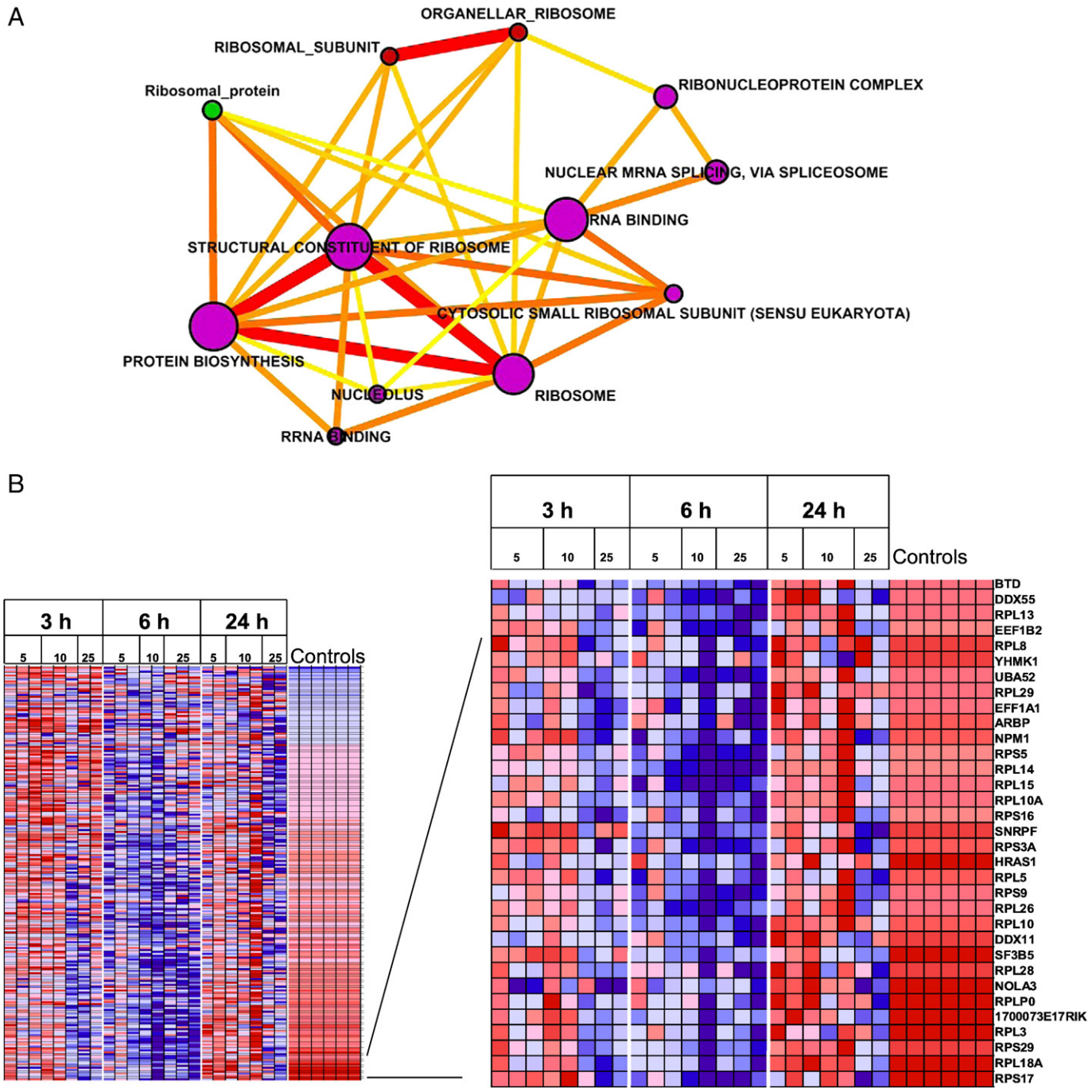

Fig. 5. DON downregulates ribosome- and protein translation-related genes. (A) Molecular concepts visualization of gene sets involved in the route for mRNA modification to protein translation. Genes from these gene sets were downregulated. This visualization method is explained in the legend of Fig. 3A. Green nodes: lymphocyte signature database; purple nodes: gene ontology. (B) Heat map of the genes from the merged gene sets of A. Downregulation of genes involved in ribosomal function was most severe after 6 h of exposure. The colors of the heat maps are explained in the legend of Fig. 3B.

downregulation was most apparent after 6 h. The expression patterns of the gene sets related to mitochondria and cytoplasm/nucleus were rather similar to that of the ribosome-related gene sets (Supplementary Figs. 8 and 9, respectively). Again many genes were upregulated after 3 h and downregulated from 6 h onwards.

Genes upregulated during negative selection of thymocytes

The finding that DON induces a T cell activation response is of high relevance, since T cell activation in the thymus induces apoptosis and rapid depletion of the activated thymocyte (Starr et al., 2003). This

Fig. 4. DON affects the relative abundance of precursor T lymphocytes. (A) Bottom part of a heat map of genes highly expressed in early precursor lymphocytes, for the largest part of the double-positive stage. For this, genes of the gene sets shown in Supplementary Fig. 7B were merged. These genes were downregulated after treatment for 3 and 6 h for all doses and remained downregulated after 24 h for the highest dose. Full heat map is shown in Supplementary Fig. 7C. (B). Top part of a heat map of marker genes for late precursor T lymphocytes, showing upregulation of these genes at 3 and 6 h of treatment. After 24 h, this upregulation was less apparent for 5 and 10 mg/kg DON but was more severe for 25 mg/kg DON. Full heat map is shown in Supplementary Fig. 7E. The colors of the heat maps are explained in the legend of Fig. 3B.

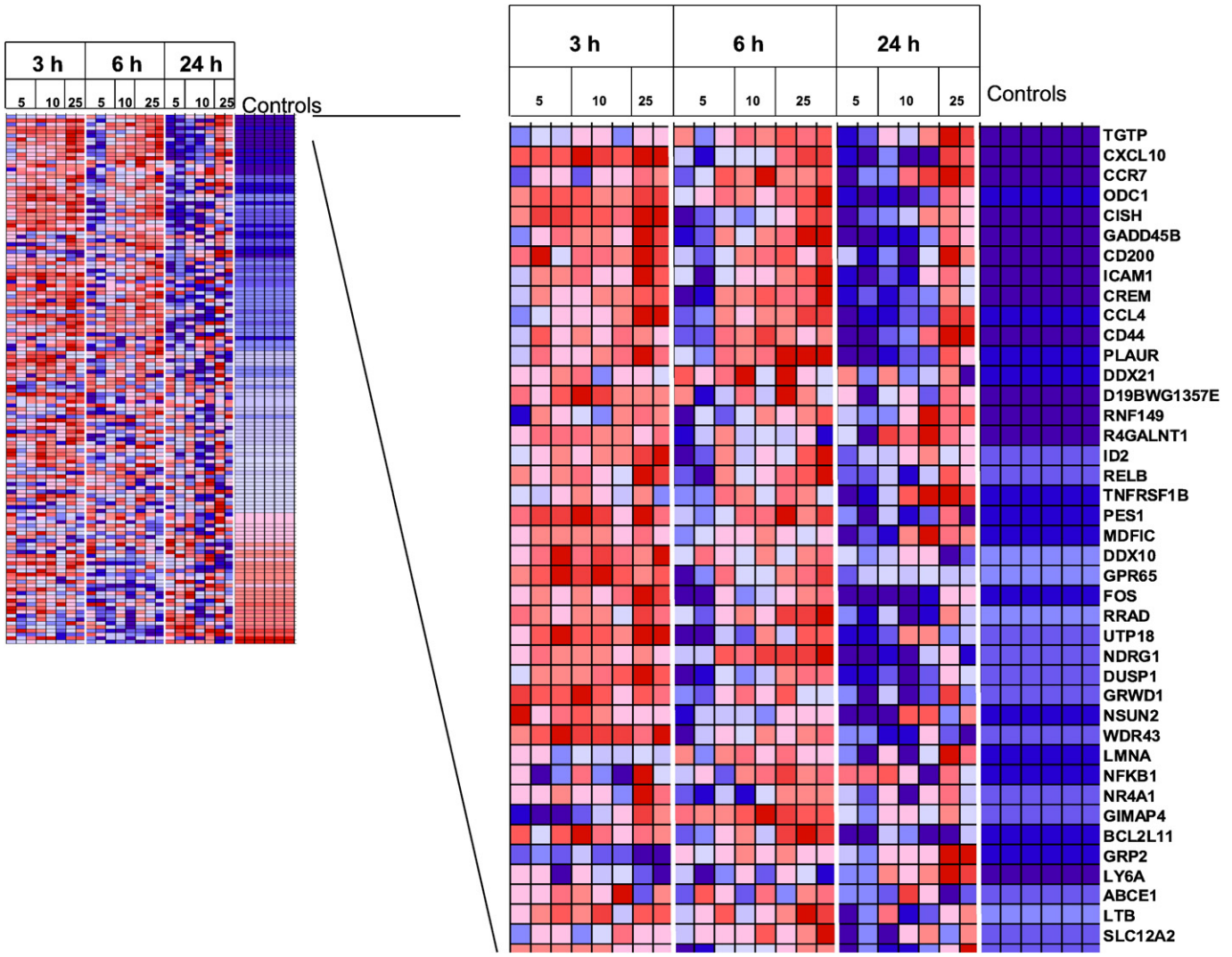

Fig. 6. Genes upregulated during negative selection of thymocytes are also upregulated by DON. Genes upregulated in double-positive thymocytes during negative selection were taken from data published by Schmitz et al. (2003) The heat map shows the effect of DON on these genes. The majority of these genes were upregulated within 3 h of DON treatment. The colors of the heat maps are explained in the legend of Fig. 3B.

process is normally induced in thymocytes that recognize "self-antigens". This selection process occurs predominantly at the double-positive stage (Starr et al., 2003). Our expression data suggest that the double-positive precursor T lymphocytes are also the main target cells of DON. These observations brought us to examine whether genes that were normally upregulated during negative selection of double-positive thymocytes are also upregulated by DON in our experiment. For this, we used a previously published gene set of 58 genes that are upregulated within 2 h in mouse double-positive thymocytes after induction of negative selection *in vivo* (Schmitz et al., 2003). From these 58 genes, 51 could be linked to our microarray data. As shown in Fig. 6, the majority of these genes were upregulated within 3 h of DON treatment as well. This indicates that DON induces molecular events similarly to those induced by negative selection on thymocytes with self-recognition.

Immunocytology

Many of the genes that are upregulated during negative selection in the thymus (Schmitz et al., 2003) are also upregulated in our experiment by DON. Negative selection in the thymus is initiated by a T cell activation response to self-antigens. This finding, therefore, further supports the involvement of T cell activation in the mode of action of DON. An essential step for T cell activation is the activation of NFAT and translocation of NFAT from the cytoplasm to the nucleus (Shaffer et al., 2001; Gwack et al., 2007). Therefore, we assessed whether DON exerts NFAT translocation in primary mouse thymocytes. As shown in Fig. 7, DON induced a rapid translocation of NFAT to the nucleus within 1 h.

Real time RT-PCR

In order to confirm the expression profiles provided by the microarray analysis, four genes were selected for expression analysis by quantitative RT-PCR. Genes were selected on basis of a key role in either T cell activation, negative selection, or ER stress response: CD86, CD80, Ccl4, and ATF3. The expression patterns of these genes as assessed by quantitative RT-PCR were very similar to those provided by the microarray analysis (Fig. 8).

Discussion

This study shows the *in vivo* effects of DON on gene expression in mouse thymus cells. Biological interpretation of the gene expression profiles confirmed some already known pathways of DON toxicity but also put forward yet unknown modes of action. Our results clearly

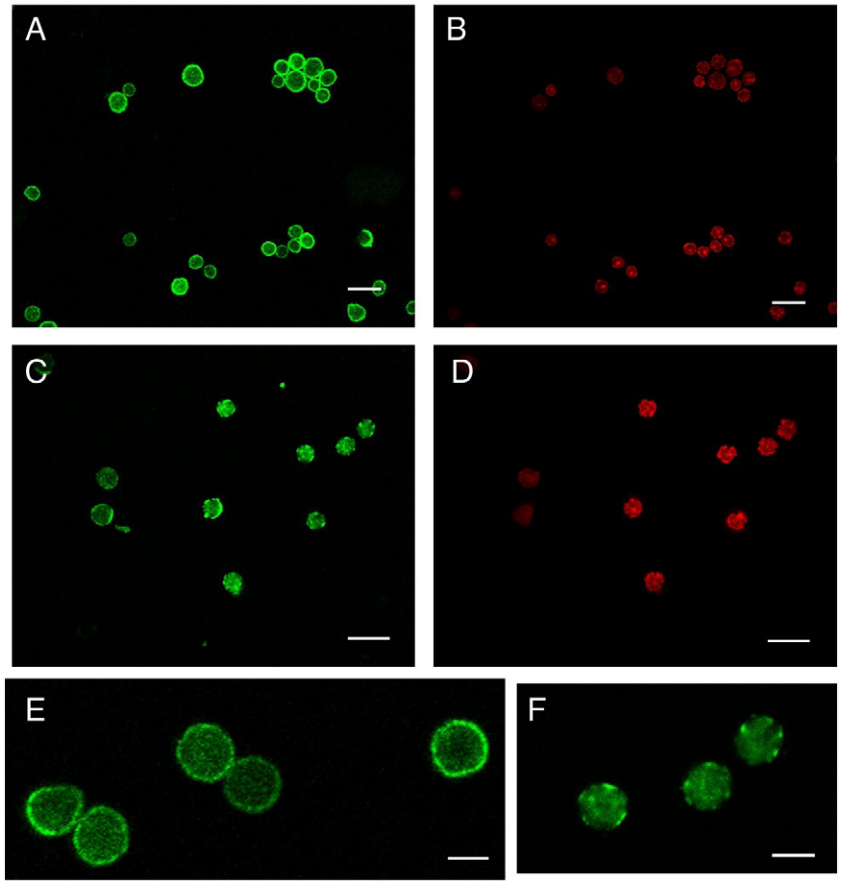

Fig. 7. Translocation of NFAT after treatment of primary thymocytes with DON. Panels A, B and E: control cells; panels C, D, and F: DON-treated cells. The green fluorescence in panels A, C, E, and F represents FITC-stained NFAT. Panels B and D show DAPI-stained nuclei. Scale bar represent 15 μm (A–D) and 5 μm (E and F).

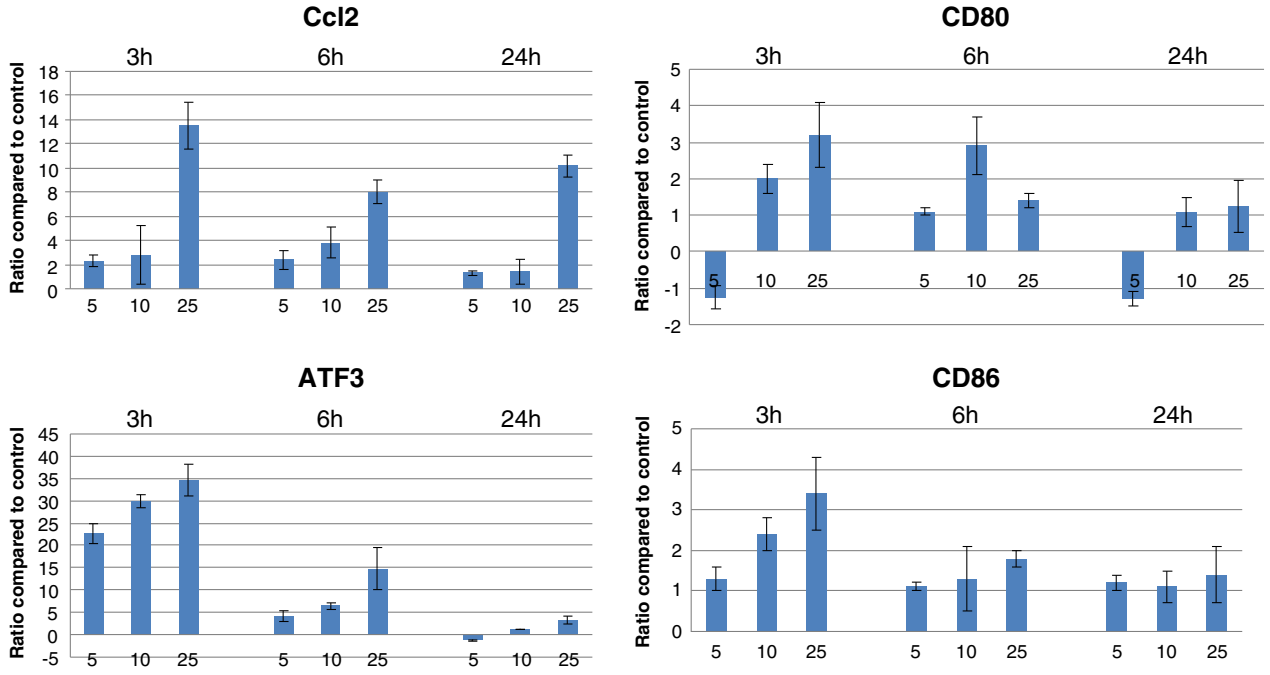

Fig. 8. Real-time PCR. RT-PCR confirmation of microarray data. Quantitative real-time PCR was performed for ATF3, CD80, CD86, and Ccl4. The expression levels of the genes are relative to Hprt1 and actB.

indicate that DON induces a T cell activation response, which is rapidly followed by apoptosis and depletion of thymocytes similarly to the process of negative selection of precursor thymocytes with self-recognition. This is in agreement with the thymus being the most sensitive target organ for DON exposure.

A high number of genes were significantly affected after 3 h of exposure at all doses used. For the 5 and 10 mg/kg bw dose groups, the number of affected genes was considerably reduced after 6 h, while only a small number of genes was still affected after 24 h. This indicates that the effects of 5 and 10 mg/kg DON were reversible. The limited period of DON toxicity is likely related to the previously described rapid metabolization and clearance of DON (Pestka, 2007; Amuzie et al., 2008). In mice treated with 5 mg/kg bw DON, concentrations have been reported to reach a maximum in plasma and tissues within 15–30 min and to be reduced by 75–90% after 120 min already (Amuzie et al., 2008). The number of affected genes induced by 25 mg/kg DON remained constant over time, indicating that this dose induces an irreversible effect, at least during a period of 24 h.

DON stimulated within 3 h the expression of many genes that are also activated during the T cell activation response. This conclusion is partly based on the similarity of our data with those on T lymphocytes that were activated with either PMA and IL2 or a combination of cytokines (Feske et al., 2001; Shaffer et al., 2001). These gene sets include calcium influx-dependent and NFkB target genes (Fig. 3A). Normally, T cell activation is induced by binding of the T cell receptor to an antigen. This induces depletion of the endoplasmatic reticulum calcium stores, which activates NFkB and evokes a larger calcium influx across the plasma membrane through calcium transporters. This rise in intracellular calcium activates calcineurin to dephosphorylate NFAT, which subsequently is translocated to the nucleus where it activates many target genes leading to T cell activation and proliferation (Gwack et al., 2007). In the present study, we were able to demonstrate using immunohistochemical techniques that DON induces translocation of NFAT from the cytoplasm to the nucleus.

Since DON is not expected to activate the T cell receptor, it likely induces one of the downstream events after T cell receptor activation. DON is known to inhibit protein synthesis by binding to the 60 S ribosomal unit where it interferes with the activity of peptidyltransferase, preventing polypeptide chain initiation, and elongation (Ueno and Hsieh, 1985; Pestka, 2008). DON like other ribosome-binding translational inhibitors also rapidly activates mitogen-activated protein kinases (MAPKs) via a process termed the “ribotoxic stress response”. These MAPKs include P38 MAPK and JNK (Pestka, 2008), which are also known to be induced during T cell activation and negative selection of thymocytes. (Rincón et al., 2000; Starr et al., 2003). Therefore, induction of MAPKs by DON might be one route leading to T cell activation. Alternatively, the action of DON on the ribosomes at the endoplasmatic reticulum might cause the endoplasmatic reticulum to release calcium leading to a T cell activation response.

T cell activation in the thymus is known to induce negative selection, and our data indicate that this process also occurs after DON exposure. Genes upregulated within 2 h after induction of negative selection of mouse double-positive thymocytes *in vivo* were also rapidly induced in our experiment by DON. The upregulation of CD40 target genes further supports this finding (Fig. 3A). CD40 and its ligand (CD40L) are master regulators of negative selection of thymocytes. CD40 regulates the expression of different co-stimuli required for negative selection like CD80, CD86, CD54, CD58, FasL, TNF, and IL-12. (Li and Page, 2001; Dong et al., 2002). Of those co-stimuli, CD54, CD80, and CD86 were significantly upregulated after 6-h exposure with 10 mg/kg bw. The upregulation of CD80 and CD86 was confirmed using real-time RT-PCR.

DON appears to induce a quick stimulus to cell activity before it exerts its toxic activity. Many gene sets related to proliferation (particularly G1–S phase), mitochondria, and ribosomes were upregulated at 3 h and highly downregulated at 6 and 24 h. This might be related to induction of T cell activation as well, which is known to quickly stimulate cells divide (Onur et al., 2009).

GSEA analysis demonstrated downregulation of genes that are highly expressed in early-precursor T lymphocytes of DN3 to double-positive stage and upregulation of genes that are highly expressed in very early or late-precursor T lymphocytes. The most likely explanation for this finding is that early-precursor T lymphocytes of DN3 to double-positive stage are more vulnerable for DON treatment than the late precursor cells. This agrees with previously published findings in mice that 12.5 mg/kg DON to induce a decrease of the number of double-positive cells within 12 h, whereas the number of late precursor cells (either $CD4^+$, $CD8^-$, or $CD4^-$, $CD8^+$) remained constant (Islam et al., 2003). The high sensitivity of double-positive cells agrees with the presently proposed role of T cell activation in mediating the toxic activity of DON. In the normal thymus, depletion of precursor T lymphocytes that respond to auto-antigens occurs at the double-positive stage as well (Starr et al., 2003). Therefore, double-positive T cells will be much more sensitive for DON-induced T cell activation than the very early or late precursor T cells.

Genes encoding proteins for cellular components as mitochondria, ribosomes, and cytoplasm/nuclei were downregulated by DON. It is tempting to relate the downregulation of ribosome- and protein translation-related genes to the ribotoxic stress response. Since mitochondria- and cytoplasm/nuclei-related genes are downregulated as well, these findings are more likely correlated to the depletion of early lymphocytes that have a higher metabolization rate than the thymus epithelial and stromal cells. Likewise, the upregulation of genes related to cell adhesion and cytoskeleton is most likely due to the relative increase of the proportion of stromal cells.

In relation to the toxic effect of DON, it is surprising that the expression data provide little indications for induction of apoptosis. This agrees, however, with previously published data showing that after 12-h treatment with 12.5 mg/kg DON less than 0.5% of the $CD4^+$ $CD8^+$ cells have apoptotic (subdiploid) nuclei (Islam et al., 2003). At this same time point, however, 25% of the $CD4^+$ $CD8^+$ cells are depleted from the thymus. Therefore, depletion of DON-affected cells likely precedes induction of apoptosis, meaning that there were apoptotic cells present in the thymus, but before the end of the treatment period, those cells were already depleted from the thymus. This rapid depletion likely occurs via phagocytosis, which agrees with our findings of a fast invasion of leucocytes and macrophages into the DON-treated thymus. Deletion via phagocytosis is also found during negative selection in the thymus (Sun and Shi; Elliott et al., 2009).

In summary, the present findings indicate that DON induces cellular events that also occur after activation of the T cell receptor, such as release of calcium from the endoplasmatic reticulum. This T cell activation is rapidly followed by negative selection of thymocytes, particularly those at the double-positive stage. At lower exposure levels (5 and 10 mg/kg), this effect is reversible, while it is irreversible at least 24 h after exposure to 25 mg/kg. This provides a plausible explanation for the high sensitivity for DON of immune cells, above all thymocytes, compared to other cell types.

Supplementary materials related to this article can be found online at doi:10.1016/j.taap.2010.11.001.

Acknowledgments

The authors thank Hakan Baykus, Jenneke Riethoff-Poortman, and Norbert de Ruijter for their technical support and Wilma Blauw and Bert Weijers of the Small Animal Center of Wageningen University (Wageningen, The Netherlands).

Sandra W.M van Kol is recipient of grant MFA6809 from the Dutch technology foundation STW.

References

Amuzie, C.J., Harkema, J.R., Pestka, J.J., 2008. Tissue distribution and proinflammatory cytokine induction by the trichothecene deoxynivalenol in the mouse: comparison of nasal vs. oral exposure. Toxicology 248, 39–44.

Azconaolivera, J.I., Ouyang, Y., Murtha, J., Chu, F.S., Pestka, J.J., 1995. Induction of cytokine mrnas in mice after oral exposure to the trichothecene vomitoxin (deoxynivalenol): relationship to toxin distribution and protein synthesis inhibition. Toxicol. Appl. Pharmacol. 133, 109–120.

Bar-Joseph, Z., Siegfried, Z., Brandeis, M., Brors, B., Lu, Y., Eils, R., Dynlacht, B.D., Simon, I., 2008. Genome-wide transcriptional analysis of the human cell cycle identifies genes differentially regulated in normal and cancer cells. Proc. Natl Acad. Sci. 105, 955–960.

Dong, C., Davis, R.J., Flavell, R.A., 2002. Map kinases in the immune response. Annu. Rev. Immunol. 20, 55–72.

Du, X., Tang, Y., Xu, H., Lit, L., Walker, W., Ashwood, P., Gregg, J.P., Sharp, F.R., 2006. Genomic profiles for human peripheral blood T cells, B cells, natural killer cells, monocytes, and polymorphonuclear cells: comparisons to ischemic stroke, migraine, and Tourette syndrome. Genomics 87, 693–703.

Eisen, M.B., Spellman, P.T., Brown, P.O., Botstein, D., 1998. Cluster analysis and display of genome-wide expression patterns. Proc. Natl. Acad. Sci. USA 95, 14863–14868.

Ekins, S., Bugrim, A., Brovold, L., Kirillov, E., Nikolsky, Y., Rakhmatulin, E., Sorokina, S., Ryabov, A., Serebryiskaya, T., Melnikov, A., Metz, J., Nikolskaya, T., 2006. Algorithms for network analysis in systems-ADME/Tox using the MetaCore and MetaDrug platforms. Xenobiotica 36, 877–901.

Elliott, M.R., Chekeni, F.B., Trampont, P.C., Lazarowski, E.R., Kadl, A., Walk, S.F., Park, D., Woodson, R.I., Ostankovich, M., Sharma, P., Lysiak, J.J., Harden, T.K., Leitinger, N., Ravichandran, K.S., 2009. Nucleotides released by apoptotic cells act as a find-me signal to promote phagocytic clearance. Nature 461, 282–286.

Feske, S., Giltnane, J., Dolmetsch, R., Staudt, L.M., Rao, A., 2001. Gene regulation mediated by calcium signals in T lymphocytes. Nat. Immunol. 2, 316–324.

Forsell, J.H., Jensen, R., Tai, J.H., Witt, M., Lin, W.S., Pestka, J.J., 1987. Comparison of acute toxicities of deoxynivalenol (vomitoxin) and 15-acetyldeoxynivalenol in the B6C3F1 mouse. Food Chem. Toxicol. 25, 155–162.

Gwack, Y., Feske, S., Srikanth, S., Hogan, P.G., Rao, A., 2007. Signalling to transcription: store-operated Ca^{2+} entry and NFAT activation in lymphocytes. Cell Calcium 42, 145–156.

Hoffmann, R., Bruno, L., Seidl, T., Rolink, A., Melchers, F., 2003. Rules for gene usage inferred from a comparison of large-scale gene expression profiles of T and B lymphocyte development. J. Immunol. 170, 1339–1353.

Islam, Z., King, L.E., Fraker, P.J., Pestka, J.J., 2003. Differential induction of glucocorticoid-dependent apoptosis in murine lymphoid subpopulations in vivo following coexposure to lipopolysaccharide and vomitoxin (deoxynivalenol). Toxicol. Appl. Pharmacol. 187, 69–79.

Kinser, S., Jia, Q., Li, M., Laughter, A., Cornwell, P., Corton, J.C., Pestka, J., 2004. Gene expression profiling in spleens of deoxynivalenol-exposed mice: immediate early genes as primary targets. J. Toxicol. Environ. Health A 67, 1423–1441.

Li, R., Page, D.M., 2001. Requirement for a complex array of costimulators in the negative selection of autoreactive thymocytes in vivo. J. Immunol. 166, 6050–6056.

Lyons, P., Koukoulaki, M., Hatton, A., Doggett, K., Woffendin, H., Chaudhry, A., Smith, K., 2007. Microarray analysis of human leucocyte subsets: the advantages of positive selection and rapid purification. BMC Genomics 8, 64.

Onur, B., Sven, L., Carsten, K., Jonathan, S., 2009. Homeostatic proliferation and survival of naïve and memory T cells. Eur. J. Immunol. 39, 2088–2094.

Pellis, L., Franssen-van Hal, N.L.W., Burema, J., Keijer, J., 2003. The intraclass correlation coefficient applied for evaluation of data correction, labeling methods, and rectal biopsy sampling in DNA microarray experiments. Physiol. Genomics 16, 99–106.

Pestka, J.J., 2007. Deoxynivalenol: toxicity, mechanisms and animal health risks. Anim. Feed Sci. Technol. 137, 283–298.

Pestka, J.J., 2008. Mechanisms of deoxynivalenol-induced gene expression and apoptosis. Food Addit. Contam. A 25, 1128–1140.

Pestka, J.J., Islam, Z., Amuzie, C.J., 2008. Immunochemical assessment of deoxynivalenol tissue distribution following oral exposure in the mouse. Toxicol. Lett. 178, 83–87.

Pestka, J.J., Zhou, H.R., Moon, Y., Chung, Y.J., 2004. Cellular and molecular mechanisms for immune modulation by deoxynivalenol and other trichothecenes: unraveling a paradox. Toxicol. Lett. 153, 61–73.

Rhodes, D.R., Kalyana-Sundaram, S., Tomlins, S.A., Mahavisno, V., Kasper, N., Varambally, R., Barrette, T.R., Ghosh, D., Varambally, S., Chinnaiyan, A.M., 2007. Molecular concepts analysis links tumors, pathways, mechanisms, and drugs. Neoplasia 9, 443–454.

Richard, J.L., 2007. Some major mycotoxins and their mycotoxicoses—an overview. Int. J. Food Microbiol. 119, 3–10.

Rincón, M., Flavell, R.A., Davis, R.A., 2000. The JNK and P38 MAP kinase signaling pathways in T cell-mediated immune responses. Free Radic. Biol. Med. 28, 1328–1337.

Robbana-Barnat, S., Lafarge-Frayssinet, C., Cohen, H., Neish, G.A., Frayssinet, C., 1988. Immunosuppressive properties of deoxynivalenol. Toxicology 48, 155–166.

Rotter, B.A., Prelusky, D.B., Pestka, J.J., 1996. Toxicology of deoxynivalenol (vomitoxin). J. Toxicol. Environ. Health 48, 1–34.

Schmitz, I., Clayton, L.K., Reinherz, E.L., 2003. Gene expression analysis of thymocyte selection in vivo. Int. Immunol. 15, 1237–1248.

Shaffer, A.L., Rosenwald, A., Hurt, E.M., Giltnane, J.M., Lam, L.T., Pickeral, O.K., Staudt, L.M., 2001. Signatures of the immune response. Immunity 15, 375–385.

Shannon, P., Markiel, A., Ozier, O., Baliga, N.S., Wang, J.T., Ramage, D., Amin, N., Schwikowski, B., Ideker, T., 2003. Cytoscape: a software environment for integrated models of biomolecular interaction networks. Genome Res. 13, 2498–2504.

Smid, M., Dorssers, L.C.J., Jenster, G., 2003. Venn mapping: clustering of heterologous microarray data based on the number of co-occurring differentially expressed genes. Bioinformatics 19, 2065–2071.

Starr, T.K., Jameson, S.C., Hogquist, K.A., 2003. Positive and negative selection of T cells. Annu. Rev. Immunol. 21, 139–176 (Epub 2002 Oct 2016).

Su, A.I., Wiltshire, T., Batalov, S., Lapp, H., Ching, K.A., Block, D., Zhang, J., Soden, R., Hayakawa, M., Kreiman, G., Cooke, M.P., Walker, J.R., Hogenesch, J.B., 2004. A gene atlas of the mouse and human protein-encoding transcriptomes. Proc. Natl. Acad. Sci. USA 101, 6062–6067.

Subramanian, A., Tamayo, P., Mootha, V.K., Mukherjee, S., Ebert, B.L., Gillette, M.A., Paulovich, A., Pomeroy, S.L., Golub, T.R., Lander, E.S., Mesirov, J.P., 2005. Gene set enrichment analysis: a knowledge-based approach for interpreting genome-wide expression profiles. Proc. Natl. Acad. Sci. USA 102, 15545–15550.

Sun, E.W., Shi, Y.F., 2001. Apoptosis: the quiet death silences the immune system. Pharmacol. Ther. 92, 135–145.

Tusher, V.G., Tibshirani, R., Chu, G., 2001. Significance analysis of microarrays applied to the ionizing radiation response. Proc. Natl. Acad. Sci. USA 98, 5116–5121.

Ueno, Y., Hsieh, D.P.H., 1985. The toxicology of mycotoxins. Crit. Rev. Toxicol. 14, 99–132.

Whitfield, M.L., Sherlock, G., Saldanha, A.J., Murray, J.I., Ball, C.A., Alexander, K.E., Matese, J.C., Perou, C.M., Hurt, M.M., Brown, P.O., Botstein, D., 2002. Identification of genes periodically expressed in the human cell cycle and their expression in tumors. Mol. Biol. Cell 13, 1977–2000.

Zhou, H.R., Yan, D., Pestka, J.J., 1997. Differential cytokine mRNA expression in mice after oral exposure to the trichothecene vomitoxin (deoxynivalenol): dose response and time course. Toxicol. Appl. Pharmacol. 144, 294–305.